Japanese Journal of Applied Physics **50** (2011) 071603 **REGULAR PAPER**
DOI: 10.1143/JJAP.50.071603

Electrical Characterization of Terphenyl-Based Molecular Devices

Touichiro Goto*, Hiroshi Inokawa[1], Yukinori Ono, Akira Fujiwara, and Keiichi Torimitsu

NTT Basic Research Laboratories, NTT Corporation, Atsugi, Kanagawa 243-0198, Japan
[1]*Research Institute of Electronics, Shizuoka University, Hamamatsu 432-8011, Japan*

Received March 11, 2011; revised April 8, 2011; accepted April 18, 2011; published online July 20, 2011

The electrical characteristics of phenylene-based molecular devices were assessed. The device consisted of nanogap electrodes and phenylene-based conjugated molecules. One nanogap electrode was obtained by the electromigration of a Au nanowire modified with a self-assembled monolayer (SAM) of 4,4-*p*-terphenyldithiol (TPDT). The other nanogap electrode was fabricated by the shadow evaporation of metals and subsequent deposition of SAM. Some devices obtained by the electromigration of Au nanowire modified with SAMs exhibited a large activation energy of electrical conduction of up to 0.26 eV. This large activation energy coincides with the intramolecular barrier estimated by *ab initio* molecular orbital calculations. On the other hand, the devices composed of shadow evaporated nanogaps and subsequently deposited TPDT exhibited a comparatively small activation energy. Neither device showed a clear gate effect with an electrical field up to 3 MV/cm. These results indicate that the electrical characteristics of molecular devices are affected by the fabrication process and the resultant molecule-electrode configuration. © 2011 The Japan Society of Applied Physics

1. Introduction

A single-molecular device (SMD) is a nanodevice that utilizes the physical properties of single molecules. An SMD is typically composed of a conductive molecule and electrodes on a gate-insulating layer. Both ends of the molecule in the SMD are connected to electrodes via chemical bonding or physical adsorption. In general, the size of the molecule for SMD is of the order of a few nanometers. The accommodation of such a small molecule requires nanogap electrodes corresponding to the length of the molecule. Such nanogap electrodes are difficult to fabricate with conventional lithography techniques. Various techniques have been employed to produce nanogaps including electromigration,[1,2] mechanical breakage,[3,4] shadow evaporation[5,6] and electrochemical platings.[7,8] Recent studies of phenylene molecules revealed that STM (Au tip and Au surface)[9] and Au nanogap electrodes[10] have different conductance characteristics. It is noteworthy that the same molecules have different electrical characteristics in different junction structures.

However, the relationship between device structures and their electrical characteristics is not well understood. An intriguing way to identify the characteristics of molecules in SMDs and the effects of nanogap electrode structures is to study SMDs with different types of nanogap electrodes. In this report, the effect of device structure on electrical conduction is investigated using two types of nanogap electrodes; one is obtained by the electromigration of Au wire and the other by the shadow evaporation of metals. A phenylene-based molecule with a large steric hindrance is selected in the expectation of producing a larger effect with electrode structures.

2. Experiment

2.1 Nanogap electrodes obtained by electromigration of Au nanowire

Two types of nanogap electrodes modified with TPDT were fabricated. One nanogap was obtained by the electromigration of Au nanowire, and the other by the shadow evaporation of metals. First, we describe the fabrication of Au nanowire.

We employed the widely-used electromigration technique,[1,2] so here we provide only a brief summary. In the first step, a 120-nm-thick gate-insulating layer was obtained by the thermal oxidation of a Si wafer. Then, contact pads for external connection were defined by the deposition of Ti (3 nm thick) and Au (200 nm thick), and then a 15-nm-thick and typically 100-nm-wide and 200-nm-long Au wire without a Ti underlayer was fabricated by vacuum evaporation and liftoff. As a molecule, we employed 4,4′-*p*-terphenyldithiol (TPDT),[11,12] which is one of the simplest oligophenyls and a model molecule with the characteristics of poly(*p*-phenylene), a typical conjugated polymer with a non-degenerate ground state.[13]

Self-assembled monolayers (SAMs) of TPDT were formed on Au surface by immersing the samples in TPDT solutions (1 mM in dehydrated tetrahydrofuran) in an Ar atmosphere for 60 min.

After the immersion, electromigration and electrical measurements were performed in a vacuum of 10^{-5} Pa. Henceforth, we refer to nanogaps obtained by the electromigration of Au nanowire modified with SAMs as electromigrated (EM) nanogaps. Although SAM formation after the electromigration of Au nanowire is ideal because the electrical characteristics before and after SAM formation can be evaluated, nanogaps without SAM formation tend to become insulated at room temperature, and conductance cannot be subsequently altered by SAM formation. This is probably due to the widening of the gap distance caused by the surface energy of the Au nanostructure with a large curvature.[14] Therefore, electromigration was performed after SAM formation on the Au surface.

The drain current–drain voltage (I_d–V_d) characteristics of the devices were mostly measured at 20 K, except for the assessment of temperature dependence.

2.2 Nanogap electrodes obtained by shadow evaporation of metals

A detailed description of the nanogap electrode fabrication technique by shadow evaporation can be found elsewhere.[5,6,11] A 20-nm-thick gate-insulating layer was obtained by thermally oxidizing a Si wafer. The first metal layer (2.5-nm-thick Ti and 12.5-nm-thick Au) and the second metal layer (25-nm-thick Au) were deposited on the oxidized Si surface at 45 and −45° with respect to the

*E-mail address: goto.touichiro@lab.ntt.co.jp

 © 2011 The Japan Society of Applied Physics

substrate normal through the patterned mask. Some electrically shorted contacts were converted to nanogap electrodes by the electromigration technique mentioned above. The SAM formation and electrical measurement procedures are the same as those mentioned in the previous section. However, it should be noted that for nanogap electrodes obtained by shadow evaporation, the SAM was formed after the fabrication of the nanogaps. The shadow-evaporated nanogaps can be evaluated by measuring the conductance before and after SAM formation. Henceforth, we refer to the molecular devices with nanogap electrodes obtained by shadow evaporation as (SE) nanogaps.

3. Results and Discussion

The electromigration of the Au nanowire started at around 0.5 V, and the wire was completely broken at ~0.8 V. After the electromigration, the initial conductance of 10–20 mS of the Au wire decreased typically to 1 μS or less. Electromigration was attempted for over 100 Au nanowires, but some of the nanowires were initially broken probably due to fabrication failure. As a result, 39 nanogaps were obtained from the Au nanowires. Figure 1(a) is a histogram of the resistances of nanogap electrodes with TPDT for a drain voltage (V_d) of 0.5 V at 20 K. As shown in Fig. 1(a), 25 nanogaps out of 39 exhibited a resistance of 10^6 to 10^8 Ω. This result is comparable to that of Danilov *et al.* who reported the resistance of single-molecular devices using oligophenylenevinylene derivatives, which has three phenylene groups like TPDT.[15] Figure 1(b) shows representative I_d–V_d characteristics of EM nanogaps for gate voltages (V_g) of 0, +40, and −40 V. Although the magnitude of I_d decreased slightly at $V_g = +40$ V (= 3 MV/cm), no clear gate effect was observed, probably due to the molecular placement in the deep gap and the large thickness of the gate oxide.

The temperature dependence of the drain current was evaluated to identify the effect of the molecules. The dependence was measured between 20 and 300 K.[16] Figure 2 shows Arrhenius plots of the drain current at $V_d = 50$ mV of typical EM nanogaps. According to previous studies, the dominant current through SMDs at high and low temperatures for small drain voltages could be a temperature-dependent hopping current (I_h) and a temperature-independent tunneling current (I_t), respectively.[17,18] Hopping conduction follows an Arrhenius equation; $I_h = A_h V_d \exp(-E_a/k_B T)$.[18,19] Here, A_h is a proportionality constant, E_a is the activation energy and k_B is the Boltzmann constant. The temperature dependence of the conductance was fitted to $I_h + I_t$. Some devices involve an additional thermally-activated conduction process with a small activation energy, in addition to $I_h + I_t$. However, the present discussion only focuses on the process with a larger activation energy. The activation energies of EM 1–3 exhibited values of 0.24–0.26 eV. These values are clearly large and probably reflect the effect of the molecular structure.

To investigate the effect of TPDT in the molecular devices, the *ab initio* molecular orbital of TPDT was calculated with the Gaussian 03 program.[20] Density functional theory (DFT) was employed as a calculation

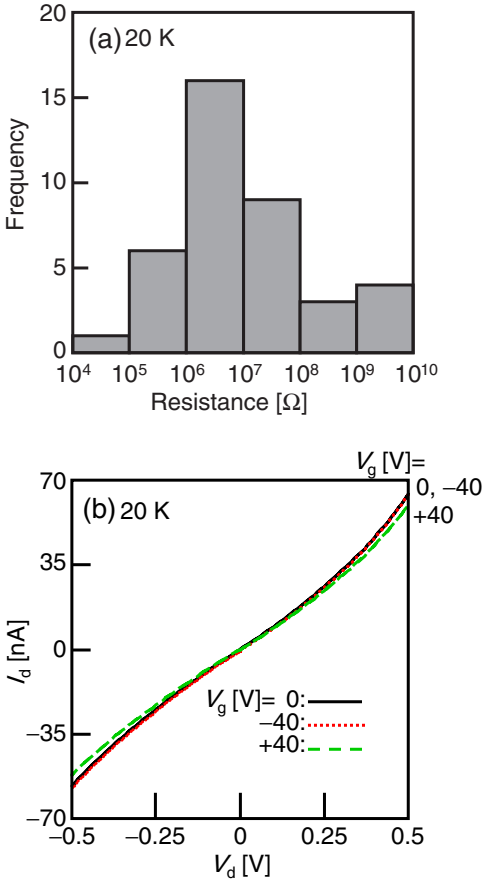

Fig. 1. (Color online) (a) Histogram of the resistances of electromigrated (EM) nanogap for $V_d = 0.5$ V at 20 K. (b) Representative I_d–V_d characteristics of EM nanogap for $V_g = -40$, 0, and +40 V at 20 K.

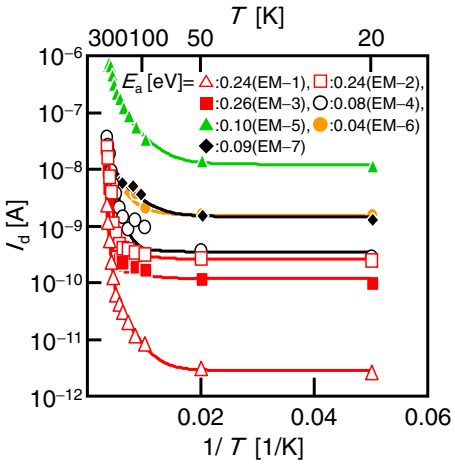

Fig. 2. (Color online) Arrhenius plots of EM nanogaps (EM 1–7) at $V_d = 50$ mV. Solid lines are fitted $I_h + I_t$–$1/T$.

method. For simplicity, the electrodes and bundling effects of SAM were neglected. All full geometry optimization calculations were performed at the B3LYP[21]/6-311+G** level.

Although *p*-terphenyl structure molecules have several conformers, the most stable structures are helical and twisted conformations (Fig. 3).[13,22] The helical conformation has

© 2011 The Japan Society of Applied Physics

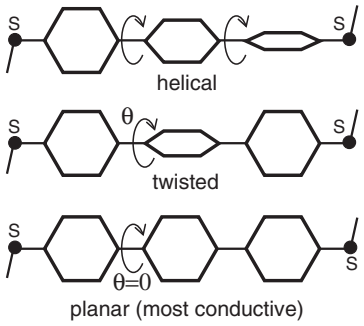

Fig. 3. Twisted, helical and planar structures of 4,4′-*p*-terphenyldithiol (TPDT). θ is the rotation angle of the phenylene group.

two arbitrary rotation angles of the phenylene group while the twisted conformation has one arbitrary angle. The theoretical calculation showed an energy difference of only 32 μeV and almost the same energy levels of highest occupied molecular orbital (−5.8 eV) and lowest unoccupied molecular orbital (−1.5 eV) between those two conformers. Considering the degree of similarity with the most conductive planar structure, we selected a twisted conformer with one arbitrariness for the calculation of the molecular structure and its electron energy. The theoretical calculation showed that the twisted conformer is most stable at a rotation angle (θ) of 38°. To analyze the relationship between rotation angles and their energy, we evaluated the structure of $\theta = 0°$ (Fig. 3), which is the most conductive structure due to the delocalization of π orbitals over TPDT. From the energy difference of TPDT structures with $\theta = 0$ and 38°, the rotation barrier for changing the most stable structure to a conductive structure was found to be 0.22 eV. This value is obviously large and indicates that TPDT has a large steric hindrance. The activation energies of EM 1–3 are in good agreement with this TPDT rotation barrier (0.22 eV) estimated by theoretical calculation. Therefore, it is considered that the rotation barrier of the phenylene group comprises the intramolecular hopping barrier and dominates the conduction at high temperature.[17] It is worth noting that, in a certain class of molecules including TPDT, steric hindrance plays an important role in the electrical conduction.

On the other hand, the theoretical calculation could not explain other activation energies of 0.04–0.1 eV (SE 4–7). The origin of these conductions with a small activation energy may be due to the granular metal surface.[23] Since electromigration forms a nanogap by breaking the metal nanowire, the nanogap surface is usually rough. The rough metal surface consists of grains that act as protrusions providing various tunneling paths and deforming the SAM structure. The SAM deformation yields intermolecular hopping, in addition to intramolecular hopping. Therefore, various current paths caused by the protrusions on the metal surface yield a small activation energy. Other possibilities are the effects of Au–S bonds and the bundling of SAMs, which were not considered in the theoretical calculations. To explain the electrical characteristics more precisely, the structure of the Au surface, and the related effects of Au–S bonds, and the bundling of SAMs should be taken into consideration.[24]

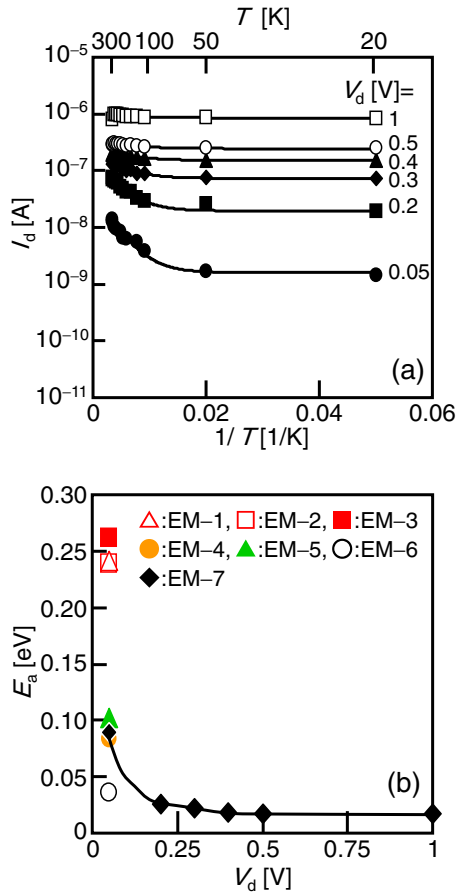

Fig. 4. (Color online) (a) Arrhenius plot of EM nanogaps for $V_d = 0.05$–1 V. Solid lines are fitted $I_h + I_t$–$1/T$. (b) E_a–V_d characteristics of EM nanogaps. The solid line for EM 7 is a guide for the eyes only.

An Arrhenius plot for one device (EM 7) could be obtained at a higher V_d [Fig. 4(a)]. Figure 4(b) shows the activation energy (E_a)–V_d characteristics of EM 7 with the data points of other EM nanogaps at $V_d = 50$ mV. As shown in Fig. 4(b), the activation energy decreases with increases in V_d. These results imply that at a higher drain voltage, the hopping conduction barrier can be lifted, and the thermal process plays a minor role.[25]

Figure 5(a) shows representative I_d–V_d characteristics of shadow-evaporated (SE) nanogap electrodes measured at 20 K before and after SAM formation.[26] After SAM formation, the conductance increased by 4–5 orders of magnitude at $V_d = 0.5$ V. Figure 5(b) is a histogram of the resistances of SE nanogaps for $V_d = 0.5$ V at 20 K. A comparison with the resistances of EM nanogaps [Fig. 1(a)] shows that the resistances of SE nanogaps tend to be about one order higher. No clear field effect in conduction was observed for a gate electric field of less than 3 MV/cm, except for those (e.g., SE 3) that exhibited Coulomb blockade characteristics at low temperature. The temperature dependence of the drain current for the SE nanogaps [Fig. 6(a)] is qualitatively similar to that for EM nanogaps. Namely, they show thermally activated conduction at high temperature and temperature-independent conduction at low temperature, and the former can be characterized by E_a, whose V_d dependence is shown in Fig. 6(b). The E_a values of all the SE nanogaps are less than 0.05 eV and seem not to

© 2011 The Japan Society of Applied Physics

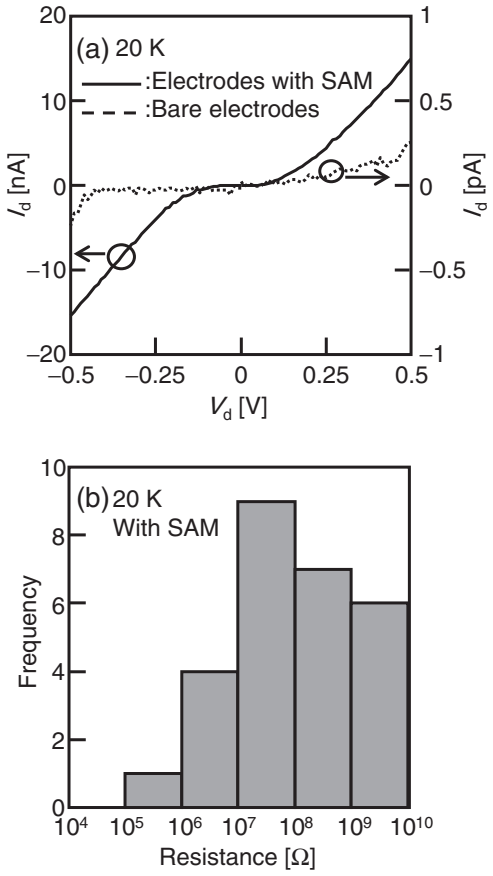

Fig. 5. (a) Representative I_d–V_d characteristics of nanogap electrodes fabricated by shadow evaporation of metals for bare electrodes and after SAM formation at 20 K. (b) Histogram of the resistances of shadow-evaporated (SE) nanogap for $V_d = 0.5$ V at 20 K.

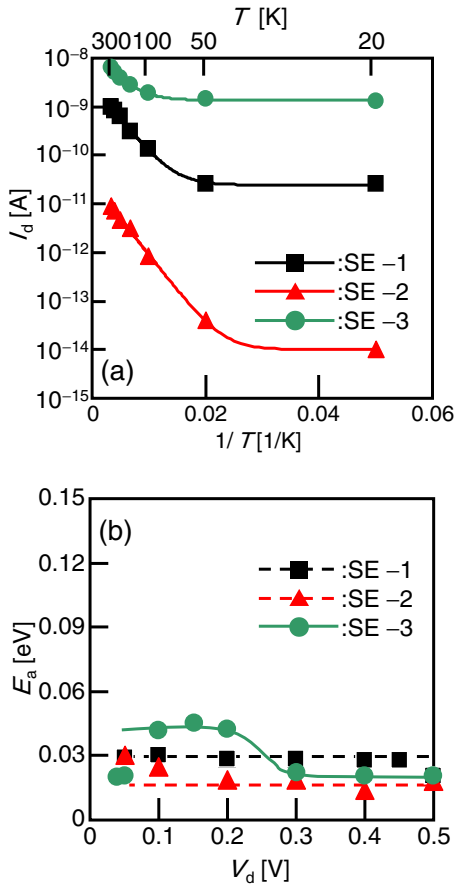

Fig. 6. (Color online) (a) Arrhenius plots of SE nanogaps (SE 1–3) at $V_d = 50$ mV. Solid lines are fitted $I_h + I_t$–$1/T$. (b) E_a–V_d characteristics of SE nanogaps. Solid (SE 3) and broken (SE 1 and 2) lines are guides for the eyes only.

reflect the intramolecular barrier of TPDT. The activation energy of SE 3, which exhibited a Coulomb blockade, decreased with increases in the drain voltage, while those of SE 1 and 2, which did not exhibit a Coulomb blockade, were almost independent of the drain voltage. The small activation energy of SE nanogaps may be related to the fabrication process and the resultant molecule-electrode configuration. Our previous study reported that the electrical characteristics of SE nanogaps can be explained on the basis of a multi-metallic-island system.[11] In short, metallic dots in nanogaps are formed during the metal evaporation and the observed electrical characteristics are related to molecule-metallic dot junctions. In fact, the SEM images revealed many metallic dots in the SE nanogaps.[11] In addition to the effect of SAM deformation mentioned previously, TPDT in SE nanogaps appears to be indirectly connected through the metallic dots in the nanogaps. This indirect connection of TPDT and electrodes also yields various current paths and could be the origin of the small activation energy.

SE 3 exhibited clear and periodic Coulomb diamond characteristics at 20 K [Fig. 7(a)]. To explain the relatively high activation energy of the SE 3 nanogap, the device was modeled as a single-electron transistor (SET), assuming that a single-electron island is metallic [Fig. 7(b)]. The SET parameters were extracted from the experimental data in Fig. 7(a) by fitting them with a compact analytical model.[27] The SET characteristics in the extended temperature range were simulated by the Monte Carlo method implemented in SIMON.[28] Figure 8(a) shows an Arrhenius plot of the SET conductance at $V_d = 10$ mV for representative gate voltages including $V_g = 0$ and $e/2C_g$ (C_g is the gate capacitance) corresponding to the Coulomb blockade and conductive conditions, respectively. The slopes on the low-temperature side (<80 K) depend on V_g. The slope for $V_g = 0$ also depends on the total capacitance C_{sum} around the SET island as shown in Fig. 8(b). On the other hand, the conductance for $V_g = e/2C_g$ is almost flat at low temperature, and gradually increases at high temperature (~300 K), indicating the transition from correlated tunneling in the two junctions at low temperature to uncorrelated tunneling at high temperature. This behavior of the conductance is very similar to the experimental behavior, and can be fitted to the superposition of thermally activated current and temperature-independent current, $I_h + I_t$, and E_a can also be extracted. Indeed, the slopes on the high-temperature side can be correlated to C_{sum} as shown in Fig. 8(c). Interestingly, not only the slopes in Fig. 8(b) but also the extracted E_a from Fig. 8(c) coincide well with the charging energy of the SET island, $E_c = e^2/2C_{sum}$ [Fig. 8(d)]. It can be concluded that the rather high E_a of SE 3, 50 meV, which is nearly equal to the E_c derived from Fig. 7(a), is a manifestation of the correlated tunneling caused by the metallic dots specific to the SE nanogap. The reason for the condition $V_g = e/2C_g$

© 2011 The Japan Society of Applied Physics

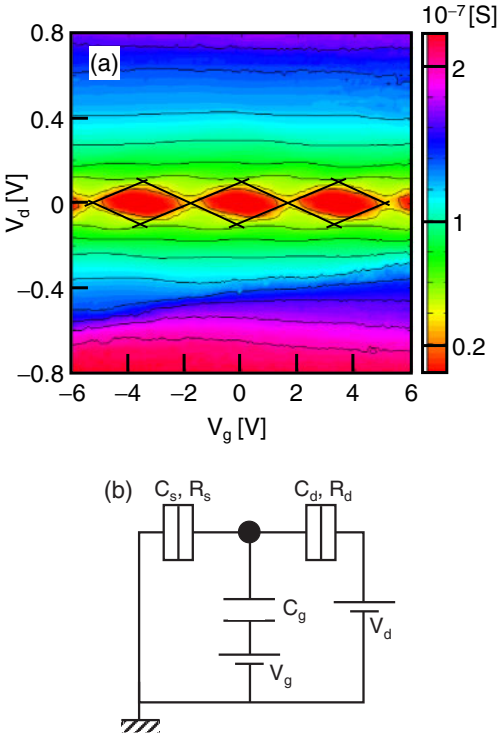

Fig. 7. (Color online) (a) Conductance contour (Coulomb diamond) plot of SE nanogaps (SE 3) in V_g and V_d plane at 20 K. Solid lines indicate the slopes of the Coulomb diamond. (b) Simulation model of single-electron transistor (SET) for analyzing experimental result for SE 3 device. Extracted parameters are $C_s = C_d = 8.0 \times 10^{-19}$ F, $C_g = 4.7 \times 10^{-20}$ F, and $R_s = R_d = 3.8 \times 10^6$ Ω.

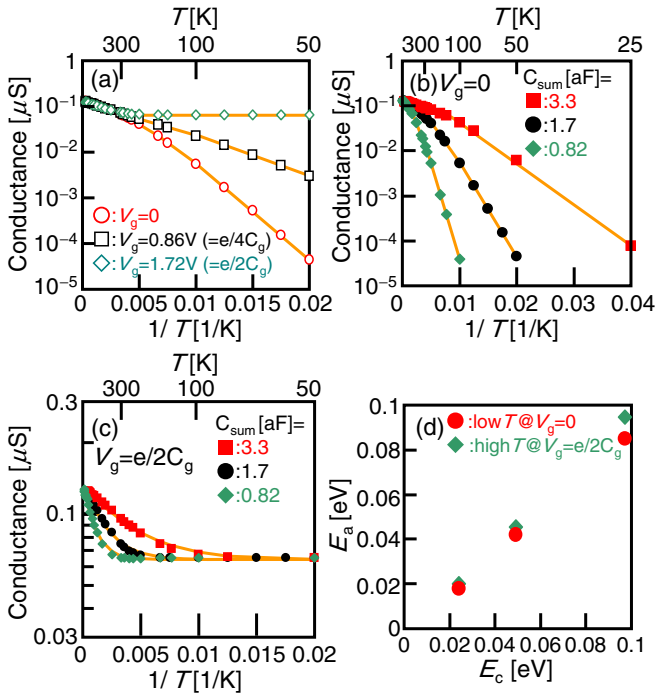

Fig. 8. (Color online) (a) Arrhenius plots of conductance at $V_d = 10$ mV for $V_g = 0$ V, 0.86 V (= $e/4C_g$) and 1.72 V (= $e/2C_g$) obtained by simulation. Arrhenius plot obtained by simulation with $C_{sum} = 0.82$ aF, 1.7 aF (corresponding to the experimental results shown in Fig. 7) and 3.3 aF for V_g = (b) 0 and (c) $e/2C_g$. Solid lines in (a)–(c) denote the fitted $I_h + I_t$–$1/T$. (d) Relationship between activation energy (E_a) and charging energy (E_c).

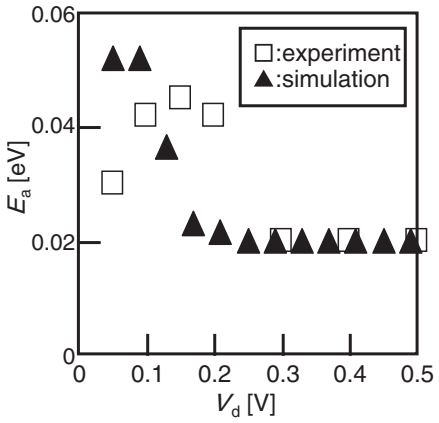

Fig. 9. E_a–V_d characteristics of shadow-evaporated nanogaps (SE 3). Plots of experiment and simulation ($V_g = 0$ V) are denoted as squares and triangles, respectively.

being realized is not clear at this moment, but, if there are SETs with various offset charges, a conductive SET should dominate the conduction in the entire system.

Figure 9 shows the E_a–V_d characteristics of an SE 3 nanogap obtained by simulation ($V_g = 0$ V) and experiment. As shown, the simulation qualitatively reproduced the E_a–V_d characteristics, thus supporting the validity of the SET model.

Our results also showed the absence of a strong gate effect. Recently, Song *et al.* demonstrated that *p*-benzenedithiol-based devices can operate as single-molecular transistors.[29] On the other hand, Lee *et al.* showed that *p*-biphenyldithiol-based devices exhibit no gate effect.[10] Considering these studies, the nanogap electrode in our work is sufficiently thick to shield the gate electric field via a thick gate insulator, and therefore, TPDT may not sense a sufficient gate electrical field. To study the gate effect of SMDs, we need a thin gate-insulating layer and thin electrodes, in addition to field-sensitive molecules.

4. Conclusions

We fabricated two types of nanogap electrodes. One was obtained by the electromigration of Au wire, and the other by the shadow evaporation of metals. Phenylene-based molecular devices were obtained by applying TPDT to these two types of nanogap electrodes. Neither type of nanogap electrode with TPDT showed a clear gate effect. An Arrhenius plot of the drain current commonly showed temperature-dependent hopping conduction at high temperature and temperature-independent tunneling conduction at low temperature.

The analysis of the Arrhenius plot showed that some electromigrated nanogaps have a larger hopping conduction activation energy, which coincides with the rotation barrier of the phenylene group inside TPDT estimated by an *ab initio* molecular orbital calculation. Shadow-evaporated nanogaps showed a comparatively small activation energy, which may be related to the fabrication process and the resultant molecule-electrode configuration. Indirect connection of TPDT and nanogap electrodes through multiple metallic dots yields various current paths, and could be the origin of the small activation energy.

© 2011 The Japan Society of Applied Physics

The relatively high activation energy of some shadow-evaporated nanogaps was explained based on the Coulomb blockade effect assuming the presence of metallic dots, which can be formed during metal evaporation and therefore are specific to the shadow-evaporated nanogaps. A simulation revealed that a rather high activation energy at a high temperature and constant conductance at a low temperature could be attributed to the single-electron tunneling effect in the conductive state, and the activation energy was related to the charging energy.

Our study encourages further investigation of the electrical conduction of molecules with a large steric hindrance and its relationship to electrode structure.

Acknowledgements

We sincerely thank Toshiaki Tamamura and Kazuhito Inokuma of NTT Advanced Technology Corporation, and Toru Yamaguchi, Katsuhiko Nishiguchi and Junzo Hayashi for support in the fabrication of the electrode devices, and Kazuaki Furukawa and Hiroshi Nakashima for SAM formation of TPDT, and Hiroyuki Kageshima for discussions about theoretical calculations.

1) H. Park, A. K. L. Lim, A. P. Alivisatos, J. Park, and P. L. McEuen: Appl. Phys. Lett. **75** (1999) 301.
2) D. R. Strachan, D. E. Smith, T. H. Park, M. J. Therien, D. A. Bonnell, and A. T. Johnson: Appl. Phys. Lett. **86** (2005) 043109.
3) M. A. Reed, C. Zhou, C. J. Muller, T. P. Burgin, and J. M. Tour: Science **278** (1997) 252.
4) R. H. M. Smit, Y. Noat, C. Untiedt, N. D. Lang, M. C. van Hemert, and J. M. van Ruitenbeek: Nature **419** (2002) 906.
5) K. Liu, Ph. Avouris, J. Bucchignano, R. Martel, and S. Sun: Appl. Phys. Lett. **80** (2002) 865.
6) M. S. M. Saifullah, T. Ondarcuhu, D. K. Koltsov, C. Joachim, and M. E. Welland: Nanotechnology **13** (2002) 659.
7) A. F. Morpurgo, C. M. Marcus, and D. B. Robinson: Appl. Phys. Lett. **74** (1999) 2084.
8) Y. Kashimura, H. Nakashima, K. Furukawa, and K. Torimitsu: Thin Solid Films **438–439** (2003) 317.
9) A. Mishchenko, D. Vonlanthen, V. Meded, M. Brkle, C. Li, I. V. Pobelov, A. Bagrets, J. K. Viljas, F. Pauly, F. Evers, M. Mayor, and T. Wandlowski: Nano Lett. **10** (2010) 156.
10) J.-O. Lee, G. Lientschnig, F. Wiertz, M. Struijk, R. A. J. Janssen, R. Egberink, D. N. Reinhoudt, P. Hadley, and C. Dekker: Nano Lett. **3** (2003) 113.
11) T. Goto, K. Degawa, H. Inokawa, K. Furukawa, K. Sumitomo, T. Aoki, and K. Torimitsu: Jpn. J. Appl. Phys. **45** (2006) 4285.
12) T. Goto, H. Inokawa, M. Nagase, Y. Ono, K. Sumitomo, and K. Torimitsu: Jpn. J. Appl. Phys. **46** (2007) 1731.
13) K. Honda and Y. Furukawa: J. Mol. Struct. **735–736** (2005) 11.
14) D. R. Strachan, D. E. Smith, M. D. Fischbein, D. E. Johnston, B. S. Guiton, M. Drndić, D. A. Bonnell, and A. T. Johnson, Jr.: Nano Lett. **6** (2006) 441.
15) A. Danilov, S. Kubatkin, S. Kafanov, P. Hedegrd, N. Stuhr-Hansen, K. Moth-Poulsen, and T. Bjrnholm: Nano Lett. **8** (2008) 1.
16) In the measurements of temperature dependence, about 20% of EM nanogaps were successfully evaluated.
17) J. Chen, L. C. Calvet, M. A. Reed, D. W. Carr, D. S. Grubisha, and D. W. Bennett: Chem. Phys. Lett. **313** (1999) 741.
18) Y. Selzer, M. A. Cabassi, T. S. Mayer, and D. L. Allara: J. Am. Chem. Soc. **126** (2004) 4052.
19) T.-T. Liang, Y. Naitoh, M. Horikawa, T. Ishida, and W. Mizutani: J. Am. Chem. Soc. **128** (2006) 13720.
20) Gaussian 03, Revision C.02 (Gaussian, Inc., Wallingford, CT, 2004).
21) A. D. Becke: J. Phys. Chem. **98** (1993) 5648.
22) K. Uchida, H. Kageshima, and H. Inokawa: Jpn. J. Appl. Phys. **44** (2005) 8759.
23) N. B. Zhitenev, A. Erbe, and Z. Bao: Phys. Rev. Lett. **92** (2004) 186805.
24) M. Brandbyge, J.-L. Mozos, P. Ordejón, J. Taylor, and K. Stokbro: Phys. Rev. B **65** (2002) 165401.
25) K. Arai, H. Endo, H. Tanaka, and T. Ogawa: Jpn. J. Appl. Phys. **43** (2004) L634.
26) Although over 200 samples were measured, electrical characteristics including temperature dependence of fewer than 10% of samples were successfully evaluated.
27) H. Inokawa and Y. Takahashi: IEEE Trans. Electron Devices **50** (2003) 455.
28) C. Wasshuber, H. Kosina, and S. Selberherr: IEEE Trans. Comput.-Aided Des. IC Syst. **16** (1997) 937.
29) H. Song, Y. Kim, Y. H. Jang, H. Jeong, M. A. Reed, and T. Lee: Nature **462** (2009) 1039.

© 2011 The Japan Society of Applied Physics